Analysis of the Chemically Reacting Laminar Boundary Layer during Hybrid Combustion

HERMAN KRIER* AND HAROLD KERZNER†
University of Illinois, Urbana-Champaign, Ill.

The chemically reacting boundary layer over a fuel plate was analyzed to show the effect of thermodynamic coupling at the solid-gas interface. The fuel is assumed to undergo surface pyrolysis with subsequent reaction with the freestream oxidizer at a flame sheet. Computed values of species and temperature profile, flame sheet and boundary-layer thickness, as well as surface blowing rates are presented for a variety of cases of stoichiometry, energy feedback, and pressure gradient. Although similarity approximations were utilized, the analysis compares favorably with results of regression studies during hybrid combustion.

Nomenclature

A = fuel surface pyrolysis constant, cm/sec [see Eq. (A9)]
B = nondimensional heat feedback ratio [see Eq. (8f)]
$\mathscr{B}$ = blowing rate parameter, proportional to f_w
c_p = specific heat of a gas species, cal/g − °K
D = mass transfer diffusion coefficient, cm²/sec
E_w = surface pyrolysis activation energy, cal/g
f = nondimensional stream function
f' = nondimensional velocity = u/u_e
h = enthalpy, cal/g
K_1 = nondimensional surface blowing parameter [see Eq. (8c)]
K_2 = nondimensional activation energy; ($K_2 = E_w/RT_e$)
L = solid fuel latent heat of vaporization, cal/g; also plate length
l = density-viscosity ratio [see Eq. (4c)]
$\dot{M}$ = mass flux rate, g/sec-cm²
$\hat{M}$ = molecular weight, g/g-mole
n = regression rate index, $\dot{r} \sim \dot{M}_{ox}{}^n$
p = pressure, atmosphere
Pr = Prandtl number = $C_p\mu/\lambda$
Q = flame heat release, cal/g
$\dot{q}$ = heat flux, cal/cm²-sec
$\dot{r}$ = fuel regression rate, cm/sec
R_L = Reynolds number, based on length; $R_L = \rho_e \mu_e L/\mu_e$
s = transformed x-component, g²/cm⁴-sec²
S_c = Schmidt number = $\mu/\rho D$
T = temperature, °K
u = x-component of velocity, cm/sec
v = y-component of velocity, cm/sec
$\dot{w}_1$ = rate of species production per unit volume, g/cm³-sec
x, y = Cartesian coordinates, cm
Y = mass fraction
α_{ox} = oxygen/fuel mole ratio at flame sheet
α_T = nondimensional heat release, $Q/C_p T_e$
β = pressure gradient parameter [see Eq. (4b)]
ζ_g = Damkohler number
η = transformed y-component [see Eq. (3)]
θ = nondimensional temperature, T/T_e
λ = thermal conductivity, cal/cm²-sec-°K
μ = absolute coefficient of viscosity
ρ = density, g/cm³
ϕ = fuel/oxygen mass ratio (stoichiometric ratio)
ψ = stream function = $(2s)^{1/2} f(\eta, s)$

Subscripts
e = boundary-layer edge
$()_\eta$ = differentiation with respect to η
$()_s$ = differentiation with respect to s
w = wall (fuel surface)
o = wall (fuel surface)
i = species index
F = fuel
ox = oxidizer
$*$ = flame sheet location
∞ = freestream conditions
p = propellant
$+$ = upper side of flame sheet
$-$ = lower side of flame sheet

Received November 27, 1972; presented as Paper 72-1144 at the AIAA/SAE 8th Joint Propulsion Specialist Conference, New Orleans, La., November 29–December 1, 1972, revision received July 2, 1973.

Index categories: Boundary Layers and Convective Heat Transfer—Laminar; Reactive Flows; Solid and Hybrid Rocket Engines.

* Associate Professor, Aeronautical and Astronautical Engineering Department. Member AIAA.

† Graduate Student, Aeronautical and Astronautical Engineering Department; presently, Associate Scientist, Thiokol Chemical Company, Brigham City, Utah.

Introduction

CHEMICALLY-REACTING flows adjacent to solid or liquid surfaces are well described within the framework of boundary-layer theory for a certain range of Reynolds numbers. A large volume of literature exists on the effects of mass transfer and chemical reactions upon boundary-layer characteristics. The reader need only study the classical monographs by L. Lees[1] and P. Chung[2] or the text by W. Dorrance[3] to determine the applicability and types of engineering problems that fall under the heading of chemically-reacting convective flows.

The particular process under consideration here is the two-dimensional multicomponent laminar boundary-layer flow shown schematically in Fig. 1. A direct application for such a reactive flow would be the problem of the hybrid combustor; one may study the review by Green[4] for a discussion of combustion in the hybrid rocket.

To analyze such a flow, let us first consider that the primary combustion zone is within the boundary layer, developed by the flow of main oxidizing gas stream past the solid surface.

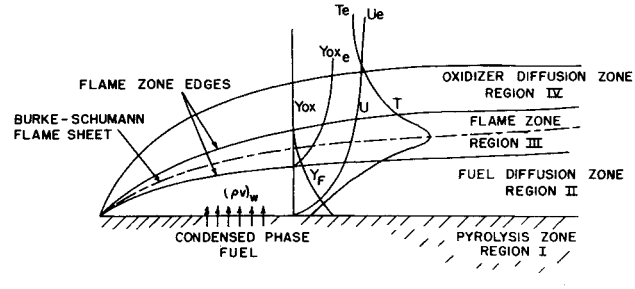

Fig. 1 Steady-state boundary-layer diffusion flame.

Oxidizer is transported to the flame by diffusion and convection from the main stream. Decomposed fuel reaches the flame by molecular diffusion and convection from the solid surface. Heat from the flame is then transmitted to the solid surface by diffusion and convection, causing the process to be self-sustaining. At the gas-solid interface, the fuel regression rate can be related to a pyrolysis law, usually equating the regression rate to a function of the instantaneous surface temperature.

As depicted in Fig. 1, there are four zones, three of which make up the gas-phase boundary layer. Tsuge and Fujiwara[5] have discussed, in terms of characteristic time variables, the four transport mechanisms required to describe hybrid combustion. These are pyrolysis (or sublimation) of fuel from the interface; diffusion of fuel and oxidizer species through the boundary layer; heat transfer from the flame within the layer; and homogeneous gas phase chemical reactions. All four transport mechanisms are to be included in the analysis that follows.

For the hybrid rocket problem, the parameter of concern is the fuel regression rate $\dot{r}$ to be determined as an eigenvalue of the boundary-layer combustion. Since by steady-state continuity

$$(\rho v)_w = \rho_p \dot{r} \tag{1}$$

then the term $(\rho v)_w$, the mass addition per unit area of the fuel vapor at the "wall," is to be predicted.

From the classical approach of laminar reactive boundary layer with mass addition (see text by Williams,[6] for example), one can show that the momentum equation admits "similar solutions" (to be discussed below) if $(\rho v)_w$ is an explicit function of length. That is

$$(\rho v)_w = \mathscr{B}(\rho_e u_e/x)^{1/2} \tag{2}$$

where the constant $\mathscr{B}$ in terms of the nondimensional stream function f is equal to $-f_w(\mu_e/2)^{1/2}$. It follows naturally that the blowing "constant" is a function of the fuel pyrolysis and therefore the wall temperature, and that this wall temperature is a function of the convective heating and flame zone location.

Governing Relations

The general conservation equations for two-dimensional laminar boundary-layer flow with chemical reactions required to describe the physics of the flow shown in Fig. 1 are detailed in Chung's monograph.[2] The Appendix summarizes those relations with a discussion of the pertinent boundary conditions.

The usual assumptions applied in the derivation of those equations are a) no body forces, b) no thermal or pressure gradient diffusion, c) no radiative energy transfer, d) specific heat of all gaseous species equal and constant, e) Fick's law for diffusion velocities applicable (the validity of Fick's law rests on the assumption of equal binary diffusion coefficients), f) steady-state flow, g) two-dimensional planar flow, h) an all gas-phase, one-step, irreversible reaction between oxidizer and fuel,‡ and i) surface pyrolysis of fuel, dependent on surface (wall) temperature.

However, the analysis will include the proper thermodynamic coupling of heat and mass transfer at the solid-gas interface; this has not been previously attempted in such a way as to predict $\dot{r}$ as an eigenvalue.

To account for compressibility, the Lees-Dorodnitsyn transformations are applied, so that

$$\eta = u_e/(2s)^{1/2}\int_0^y \rho\, dy; \quad s = \int_0^x \rho_e u_e \mu_e\, dx \tag{3}$$

As usual, y is the distance normal to the fuel plate and x is the stream-wise distance. We may also define a nondimensional stream function, f, as $f(s,\eta) \equiv \psi/(2s)^{1/2}$, so that $u/u_e = \partial f/\partial\eta$. With the continuity equation satisfied automatically by the stream function, the conservation equations of momentum, species and energy can be expressed as

‡ One could include a chemical kinetic scheme instead, as Liu and Libby[7] have done.

Momentum:

$$(lf_{\eta\eta})_\eta + ff_{\eta\eta} + \beta[\rho_e/\rho - f_\eta^2] = 2s(f_\eta f_{\eta s} - f_s f_{\eta\eta}) \tag{4a}$$

where

$$\beta = (2s/u_e)\, du_e/ds \tag{4b}$$

a constant, and

$$l \equiv \rho\mu/\rho_e \mu_e \tag{4c}$$

Species:

$$[(l/S_c)Y_{i_\eta}]_\eta + fY_{i_\eta} - \zeta_g \dot{w}_i = 2s(f_\eta Y_{i_s} - f_s Y_{i_\eta}) \tag{5}$$

Energy:

$$[(l/P_r)\theta_\eta]_\eta + f\theta_\eta + (\zeta_g Q/c_p T_e)\dot{w}_i = 2s(f_\eta \theta_s - f_s \theta_\eta) \tag{6}$$

With the usual boundary-layer assumption of constant impressed pressure, and assuming that molecular weight is constant, the equation of state is added so that

$$\rho/\rho_e = T_e/T \equiv 1/\theta \tag{7}$$

A typical expression of the source term, $\dot{w}_i$, substituted in Eqs. (5) and (6) can be found in the report by Waldman et al.[8]; a review of the meaning of the Damkohler number ζ_g is given by Chung.[9] For a majority of the calculations presented here, the equilibrium flame sheet assumption is utilized, which implies assuming infinite kinetics, i.e., infinite Damkohler number. This permits one to consider the flame zone as an infinitesimally thin mathematical surface, across which certain conservation matching can be applied; the source term of heat and mass appear only through the boundary conditions. At the flame sheet Y_F and Y_{ox} are zero.

Boundary Conditions

The Appendix summarizes the energy and mass balance at the gas-solid interface which are now expressed in terms of the stream function, species, species gradients, temperature and heat flux. The proper boundary conditions are transformed so that at $\eta = 0$

$$f_w = -[K_1 e^{-K_2/\theta_w} + 2R_L \mu_e^2 f_s] \tag{8a}$$

$$f_\eta = 0 \tag{8b}$$

Here K_1, the blowing parameter, defined as

$$K_1 = \rho_p A(2R_L)^{1/2}/\rho_e U_e \tag{8c}$$

and K_2, the surface pyrolysis activation energy, as E_w/RT_e. The species and energy matching condition give

$$Y_{i_\eta} + [f_w + 2R_L \mu_e^2 f_s](Y_i - Y_{i-}) = 0 \tag{8d}$$

$$B\theta_\eta + [f_w + 2R_L \mu_e^2 f_s] = 0 \tag{8e}$$

where

$$B = \frac{c_p l}{c_{p-}(\theta_w - \theta_p) + L + (c_{p-} - c_p)\theta_w} \tag{8f}$$

Here L is the latent heat of sublimation and θ_p is the cold fuel temperature. We also assume $Y_{i-} = 1$ (pure fuel). At the boundary-layer edge, $\eta \equiv \eta_e \to \infty$ we specify

$$f_\eta = 1 \tag{9a}$$

$$Y_i = Y_{ox_e}\text{(given)}; \quad (Y_F = 0) \tag{9b}$$

$$\theta = 1 \tag{9c}$$

Equations (4–7) can now be solved to determine the variable properties of a chemically reacting laminar boundary layer. As expected, a great difficulty in the solving of these basic partial differential equations is due to the coupling between the equations and boundary conditions.

Similarity Assumption

In order to further help simplify these complex reactive flow relations, similarity approximations have been often applied. This involved a transformation to a new coordinate system (s,η) from the original (x,y) system, where x and y are the streamwise and normal coordinates, respectively. The similarity transformation is successful if the s-variations of functions of

the dependent variables vanish or become of negligible importance, in which case the partial differential equations become ordinary differential equations. Such an approach will be used here, in light of the flame sheet approximation, although it is strictly forbidden if the wall temperature is not constant.

The primary question is "When do similar solutions adequately approximate these nonequilibrium processes?" Very few attempts have been made towards the solution of the full partial differential equations (see Chung[2]). The major difficulty is the coupling through the boundary conditions and the requirement of initial conditions on profiles at a given s-location.

To extract the essential features of the hybrid combustion processes, we have assumed that similarity is sufficient, for the time being, and therefore all derivatives with respect to s are set to zero in Eqs. (4a, 5, 6, 8d, and 8e).

The Parameters

By also setting Prandtl, Lewis, and Schmidt numbers equal to unity, great simplification is made in the solution to the conservation equations. This simplification allows us to disregard exact calculations of chemical and thermodynamic parameters.

An extensive search of the literature has indicated some effort in evaluating fluid properties in chemically reacting boundary layers. Penner and Libby[10] used a best curve fit for thermodynamic parameters and found appreciable changes in boundary-layer parameters. Such a complexity is not included here.

Even with simplification in Lewis, Schmidt, and Prandtl numbers, the conservation equations still remain coupled by the fluids property parameter l defined by Eq. (4c). The power viscosity law was used to determine the effects of the parameter l. Usually the approximation that $l = 1$ was made and therefore the fluid properties were neglected in the solution to the conservation equations.

The thermodynamic coupling at the wall is determined by the parameters B, K_1, and K_2. A detailed discussion of the range and applicability of these parameters is given in Kerzner.[11] The heat feedback ratio B should generally be less than unity; a typical value of $\frac{1}{2}$ was used throughout to reflect hybrid combustion, although comparisons will be made with a variety of heat ratios. The pyrolysis-blowing constant, K_1, varies from 10 to 1000; and pyrolysis Arrhenius constant K_2 ranged from $\frac{1}{4}$ to 10. The nondimensional gas phase heat release α_T was varied from four to ten. The pressure gradient parameter β was set to zero for most studies reported below. It is worth noting that since K_1, the blowing parameter, is a function of the length, as well as the pyrolysis constant, it should be determined from nonsimilarity conditions. The results show however the regression rate $\dot{r}$ as a function of freestream oxidizer mass fraction is weakly dependent upon K_1.

As mentioned, the unknown wall blowing rate, f_w, as well as the fuel mass fraction at the wall, Y_{Fw}, were eigenvalues of the problem, uniquely determined by the coupled boundary conditions and by solving the conservation equations for the given parameters listed above and for a given freestream oxidizer mass fraction, Y_{ox_e}.

Flame Sheet Analysis

According to the flame sheet model, the complete solution for the boundary-layer properties must consist of two solutions; region II where $0 \leqq \eta \leqq \eta_*$ and region IV where $\eta_* \leqq \eta \leqq \infty$. At the interface of these two regions, f and f' must be continuous. The oxidizer side of the flame sheet is noted as η_*^+ and the fuel side as η_*^-.

Following the procedure detailed by Libby and Pierucci[12] one can integrate the momentum, energy and species equation across the flame zone and then limit the zone to a sheet. It is easy to show that

$$\frac{-(dY_F/d\eta)_-}{(dY_{ox}/d\eta)_+} = \hat{M}_F/\hat{M}_{ox} = \phi \tag{10}$$

$$\frac{d\theta}{d\eta}(\eta_*^+) - \frac{d\theta}{d\eta}(\eta_*^-) = -\left(\frac{\alpha_T}{\alpha_{ox}}\right)\frac{dY_{ox}}{d\eta}(\eta_*^+) \tag{11}$$

where $\alpha_T \equiv Q/c_p T_e$, and $\alpha_{ox} = \hat{M}_{ox}/\hat{M}_T$.

For the case of zero pressure gradient, the governing equations can be simply stated as

Momentum: $$f_{\eta\eta\eta} + f f_{\eta\eta} = 0 \tag{12}$$

Energy: $$\theta_{\eta\eta} + f\theta_\eta = 0 \tag{13}$$

Species: $$Y_{i_{\eta\eta}} + f Y_{i_\eta} = 0 \tag{14}$$

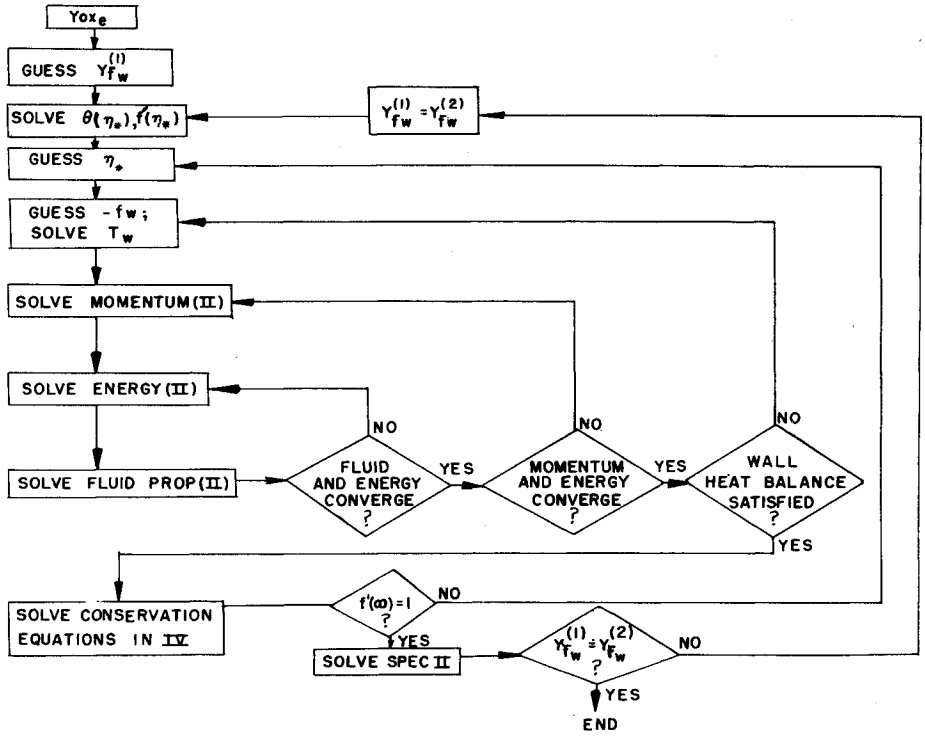

Fig. 2 Outline of numerical analysis used to solve the flame sheet combustion model.

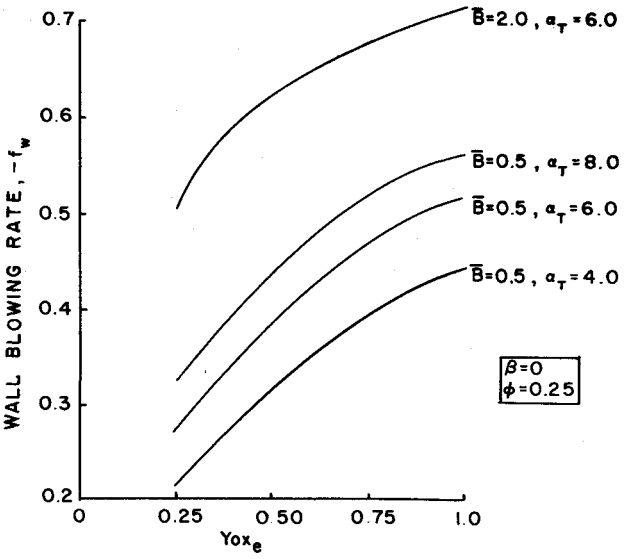

Fig. 3 Wall blowing rate vs freestream oxidizer mass fraction for variable heat release and heat ratio.

with the usual boundary conditions, that at $\eta = 0$ and with the conditions $f(o) = -K_1 \exp[-K_2/\theta(o)]$; $df/d\eta(o) = 0$; $dY/d\eta(o) = f(o)[1 - Y_F(o)]$; and $d\theta/d\eta(o) = -f(o)/B$. At the flame sheet $\eta = \eta_*$, which is determined implicitly when solving Eqs. (12–14) and including the jump conditions, equations (10–11), we also know that $Y_F(\eta_*) = Y_{ox}(\eta_*) = 0$, and that the temperature, θ, and shear, $f_{\eta\eta}$, must be continuous.

At the boundary-layer edge, $\eta \to \infty$, we state as usual that $\theta = df/d\eta = 1$ and $Y_{ox}(\infty) = Y_{ox_e}$.

Equations (12–14) can be easily integrated to Crocco type integrals, as discussed in great detail by Penner and Libby.[10] It is easy to show that

$$Y_F = Y_{F_w}[(f_*' - f')/f_*'] \tag{15a}$$

where f_*' is the velocity at the flame sheet, $\eta = \eta_*$

$$Y_{ox} = Y_{ox_e}[(f_*' - f')/f_*' - 1] \tag{15b}$$

$$f_*' = \frac{Y_{F_w}}{Y_{F_w} + \theta Y_{ox_e}} \tag{15c}$$

$$\theta_* = \theta_w + (1/B)[Y_{F_w}/(1 - Y_{F_w})] \tag{15d}$$

and

$$\theta_\eta = [f'(\theta_* - \theta_w) + f_*'\theta_w]/f_*' \qquad \eta \leqq \eta_* \tag{15e}$$

$$= [f_*' + f'(\theta_* - 1) - \theta_*]/(f_*' - 1) \qquad \eta \geqq \eta_* \tag{15f}$$

The reactive laminar boundary-layer problem is now completely specified. For a given value of Y_{ox_e} and propellant properties, unique solutions to the conservation equations are obtained.

The numerical procedure is outlined in Fig. 2; details are found in Ref. 11. A comparison of the results can now be made with other reactive boundary-layer analysis. The predictions of the wall blowing rate, wall shear stress, flame sheet velocity, flame position, boundary-layer thickness, and flame temperature are analyzed below.

Calculated Results

Figure 3 shows the predicted wall blowing function, $-f_w$, vs freestream oxidizer mass fraction as a function of amount of heat transferred to the solid (B, α_T parameters). The blowing constant K_1 was set at 50 and K_2 at 5. A discussion of relative sensitivity of these two parameters is presented later.

Quantitative comparisons of the wall blowing rate can be made with the works of Emmons[13] and Chen and Toong.[14] The model chosen by Emmons, for example, has certain important differences from the one described here. They are as follows.

1) Boundary conditions are specified at the wall and the freestream only. The oxidizer concentration goes to zero at the wall. Although a flame sheet model is "implied" by Emmons, it is never actually utilized.

2) Emmons' problem effectively decouples the momentum equation from the species and energy equations, especially with respect to the boundary conditions. Thus his solution to the wall blowing rate requires only a solution to the momentum equation.

3) The solution to the momentum equation is accomplished by assuming a value for η_∞, usually at a high enough value such that $f''(\infty) < 10^{-5}$. Although no mention of the numerical procedure is given in the Emmons work, it appears that the solutions obtained were carried out for a constant boundary-layer thickness. When the boundary-layer thickness is allowed to vary as it should in the mass injection type problems, the predictions of the blowing rate and wall shear stress will also vary.

The momentum equation is a third-order partial differential equation with four boundary conditions, the fourth one, being implied is $f''(\eta) < \varepsilon$. The fourth boundary condition is necessary to determine the total boundary-layer thickness. The method of determining the total boundary-layer thickness is accomplished by determining range of integration necessary to satisfy the first three boundary conditions, and then extend the solution until the implied fourth condition is satisfied. This technique was employed by Emmons, and Chen and Toong, an integration range of $\eta = 6$. This technique has proven satisfactory for boundary-layer flows without mass injection.

However, with mass injection, as in the present study, a larger value of η-range must be employed because of the thickening of the boundary layer due to mass injection. Changing the range of integration from $\eta = 8$ to $\eta = 6$ can produce errors in the wall blowing rate between 10–20%.

To overcome this problem, the conservation equations were solved independently in the regions above and below the flame sheet, and then matched at the flame sheet through the boundary conditions and jump conditions. By imposing boundary conditions at the wall and freestream, one can only obtain a distributed flame zone, instead of a flame sheet, without oversimplifying the problem. For each value of η-range, there will exist one value, for the flame sheet location and wall blowing rate. Therefore, without the use of the jump conditions, there may exist several values for flame sheet locations and wall blowing rates, for various η-ranges. An analysis which utilizes the flame sheet model and omits the jump conservation by assuming an erroneous value of η-range, actually violates the conservation of energy across the flame sheet. This type of result usually exhibits lower values of wall blowing rates than

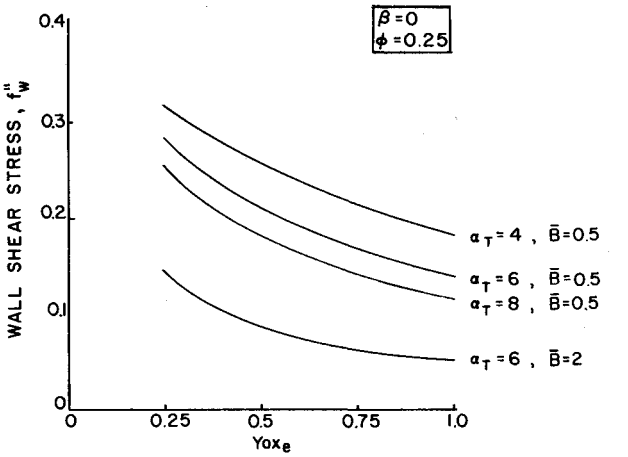

Fig. 4 Wall shear stress vs oxidizer mass fraction for variable release and heat ratio.

Table 1 Comparison of flame sheet models

$\theta = 0.25, \alpha_T = 6, \bar{B} = 2, \beta = 0, Y_{ox_e} = 0.232, K_1 = 50$

	Present study	Chen-Toong[14]	Emmons[13]
Y_{F_w}	0.76	0.63	...
$-f_w$	0.504	0.40	0.572
f_w''	0.144	0.15	0.589
η_*	3.89	3.0	...
η_∞	6.98	6.0[a]	6.0[a]
θ_*	2.74	5.7	...
θ_w	1.09	1.0[b]	...
$f'(\eta_*)$	0.925	0.90	...

[a] The edge of the boundary layer as set a priori.
[b] Always fixed.

would normally be found in variable boundary-layer thickness solution.

Table 1 indicates for a specific example the different predictions. Figures 4–6 show the predictions of the wall shear, flame height and flame temperature as the freestream oxidizer mass fraction is varied. For all cases the stoichiometric fuel-oxidizer ration, ϕ, is set at $\frac{1}{4}$.

For the case of an arbitrary finite pressure gradient, i.e., $\beta \neq 0$ the momentum equation can no longer be integrated in closed form, so that the flame velocity and temperature must be determined by iteration procedures which satisfy the jump boundary conditions at the sheet.

To simplify the numerical procedure, θ_* was chosen as an input, instead of Y_{ox_e}. Y_{ox_e} values were determined later by solving the species equation in region IV as an initial value problem, since the value and gradient of oxidizer mass fraction are defined at the flame sheet. Then a solution to boundary condition, Eq. (11), eventually yields a unique velocity and free-stream oxidizer mass fraction for any given flame temperature.

Figure 7 shows the effect of an accelerating pressure gradient on the wall blowing rate, under the constraint of a similarity solution. For the parameters listed, a pressure gradient of $\beta = 0.02$ increases the blowing rate by at least 25% for every given value of Y_{ox_e}. These results agree qualitatively with those

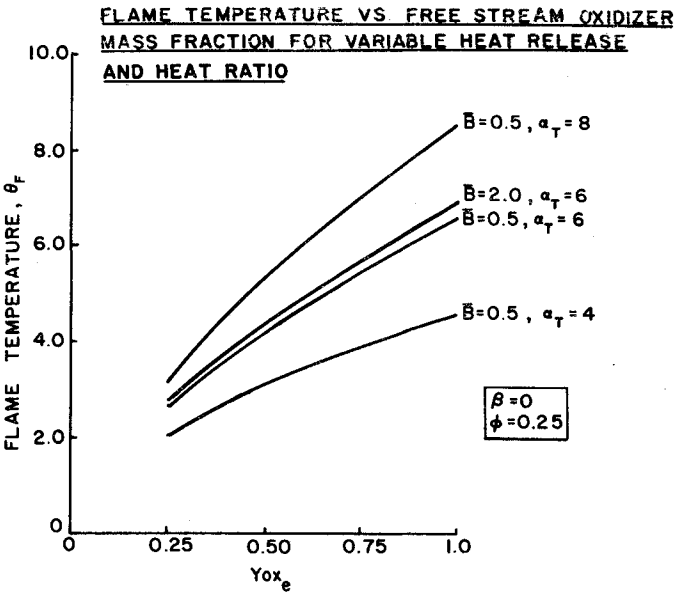

Fig. 6 Flame temperature vs oxidizer mass fraction.

presented by Chen and Toong.[14] Calculations also show, as expected that wall shear and boundary-layer thickness increase with β, while the flame height decreases. In addition velocity overshoots, i.e. ($f_*' > 1$, when $\beta > 0$) are predicted. Details are again given in Ref. 11.

Surface Regression Rate

The fuel regression rate, $\dot{r}$ (in./sec), can be calculated from the blowing rate, $-f_w$, which was shown to be a strong function of the oxidizer mass fraction, and therefore the oxidizer mass flow rate, $\dot{M}_{ox} = Y_{ox_e}\rho_e U_e$. For a given set of known thermodynamic properties, such as $\bar{B}$, ϕ, α_T, K_2 and an assumed average Reynolds number (which gives K_1), Fig. 8 shows that $\dot{r} \sim \dot{M}_{ox}^n$. The exponent n compares favorably with the experimental results of Smoot and Price,[15,16] those tabulated by Kosdon and Williams,[17] and the analytical investigation of Kumar and Stickler.[18]

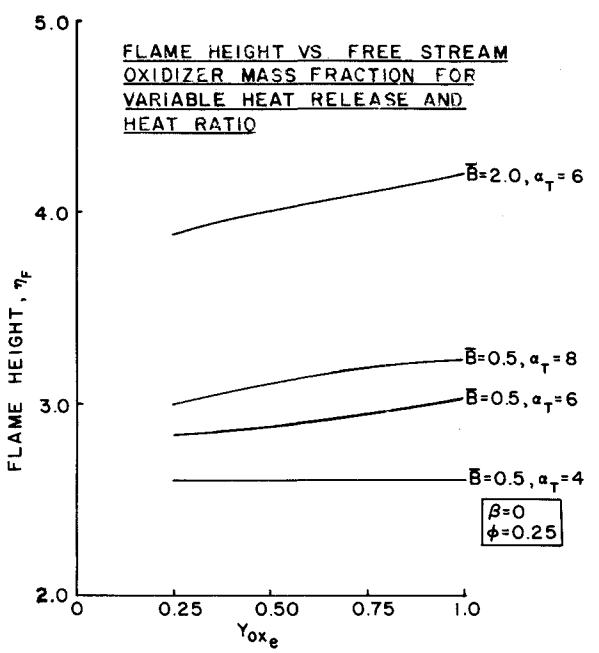

Fig. 5 Flame height vs oxidizer mass fraction.

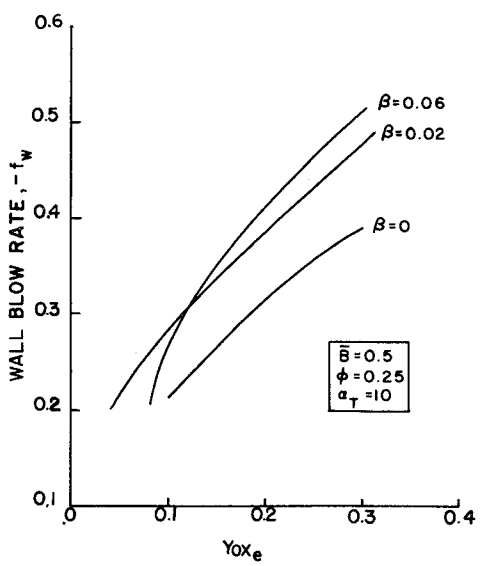

Fig. 7 Wall blowing rate vs oxidizer mass fraction for variable pressure gradient.

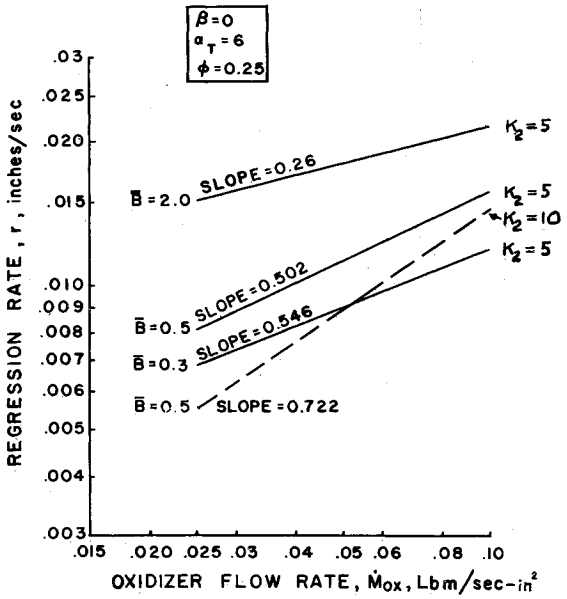

Fig. 8 Fuel regression rate vs oxidizer mass flux.

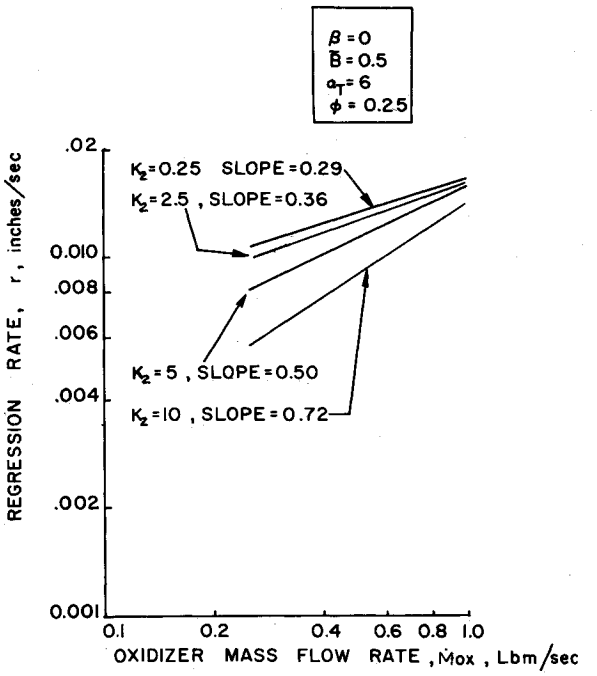

Fig. 10 Effect of pyrolysis constant on fuel regression rate-oxidizer mass flux relation.

Figure 9 indicates that the effect of K_1 (as it varies between the typical range of 20–500) on the slope n is not great, implying that for the flame sheet analysis, at least, that the similarity approximation is not a bad one.

The chemical pyrolysis property of the fuel, in terms of the activation constant K_2 is more important however, in determining the slope n. This is shown in Fig. 10.

As expected the greater the surface activation parameter K_2, the greater the sensitivity of pyrolysis rate to wall temperature and therefore eventually to the oxidizer mass fraction.

An effect of chamber pressure (P_e) on the regression rate could be added to the above predictions by simply letting either the pyrolysis pre-exponential constant A, or the surface activation parameter, K_2 be prescribed functions of pressure. Tsuge and Fugiwara[5] obtain an influence of pressure on their predicted pyrolysis rate by assuming $\theta_w = \theta_w(P_e)$, some equilibrium vapor condition. The validity of such approaches is not known and was therefore not included in our predictions.

Conclusions

We have studied the combustion of initially unmixed pyrolyzed fuels and oxidizers in a laminar boundary layer with thermodynamic coupling at the solid-gas interface, by numerically integrating the conservation equations. With certain known aerothermodynamic parameters (such as heat feedback ratio B; the stoichiometric fuel/oxygen mass ration ϕ; the diffusion flame heat release term α_T; the pyrolysis properties K_1 and K_2, where K_1 is a function of Reynolds number) it is possible to predict the fuel regression rate as a function of oxidizer mass flow rate.

Presently we are in the process of modifying the governing equations to include the turbulent flowfield processes. In another related investigation we are looking at the effect of finite rate chemistry, represented by a finite Damkohler number. Figure 11 is a typical result, showing that a Damkohler number as low as 100 predicts the equilibrium (flame sheet) blowing rate within 1% for the case studied. This would indicate that a flame sheet limit used in this study is a good approximation for the laminar reactive boundary layer. The nonsimilar equations, i.e., with the included streamwise s variation should also be studied, but the problem of unknown initial velocity, temperature, species profiles and the complexity of solving coupled nonlinear partial differential equations (instead of ordinary ones) discourages such ideas at the present.

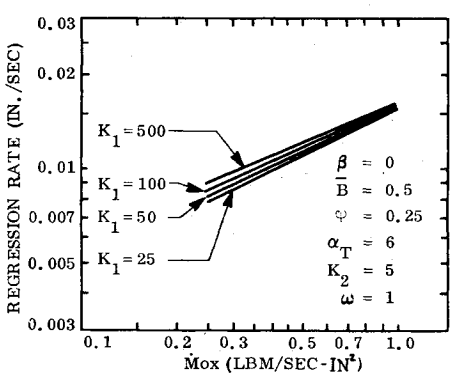

Fig. 9 Effect of blowing constant on fuel regression rate-oxidizer mass flux relation.

Appendix: Review of Reactive Boundary-Layer Governing Equations

The governing relations for chemically reacting, two-dimensional, multicomponent laminar boundary layers with the standard assumptions are:

Continuity:

$$(\partial/\partial x)(\rho u)+(\partial/\partial y)(\rho v) = 0 \tag{A1}$$

Momentum:

$$\rho\left(u\frac{\partial u}{\partial x}+v\frac{\partial v}{\partial y}\right) = -\frac{dp}{dx}+\frac{\partial}{\partial y}\left(\mu\frac{\partial u}{\partial y}\right) \tag{A2}$$

Energy:

$$\rho c_p\left(u\frac{\partial T}{\partial x}+v\frac{\partial T}{\partial y}\right)-u\frac{dp}{dx} = \frac{\partial}{\partial y}\left(\lambda\frac{\partial T}{\partial y}\right)+ \sum_{i=1}^{N}\rho D\frac{\partial Y_i}{\partial y}\frac{\partial h_i}{\partial y}+\mu\left(\frac{\partial u}{\partial y}\right)^2-\sum_{i=1}^{N}h_i\dot{W}_i \tag{A3}$$

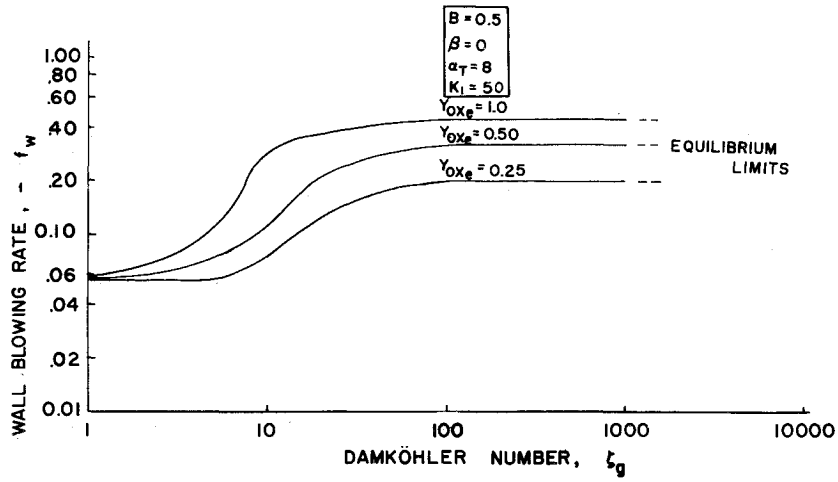

Fig. 11 Wall blowing rate vs Damkohler number for variable oxidizer mass fraction.

Species:

$$\rho\left(u\frac{\partial Y_i}{\partial x}+v\frac{\partial Y_i}{\partial y}\right)=\frac{\partial}{\partial y}\left(\rho D\frac{\partial Y_i}{\partial y}\right)+\dot{W}_i \tag{A4}$$

State:

$$P=\rho RT\sum_{i=1}^{N}(Y_i/\hat{M}_i) \tag{A5}$$

where

$$h_i=h_i^0+\int C_p\,dT$$

Boundary Conditions at Solid-Gas Interface ($y=0$)

From the usual boundary-layer analyses and the mass and energy balance the proper boundary conditions are derivable such that at $y=0$:

$$u=u_w=0 \tag{A6a}$$

$$v=v_w=\dot{r}(\rho_p/\rho_w)\ \text{(in terms of unknown regression rate)} \tag{A6b}$$

$$Y_i=Y_{F_w}\ \text{(unknown species fraction)} \tag{A7a}$$

$$T=T_w\ \text{(unknown wall temperature)} \tag{A7b}$$

Often in problems including surface chemical reactions, the surface mass injection rate $\dot{r}$ is controlled by the net surface chemical reaction rate. Thus the surface distribution of reacting species Y_{F_w} is not known a priori, unless the surface is known to be in chemical equilibrium. Since vaporizing surfaces are generally not characterized by chemical equilibrium, boundary conditions (A7a) must be coupled to a mass balance expression at the solid-gas interface.

At the wall (solid-gas interface), the component i is transported from the gas to the solid by diffusion at the rate of $(\rho D^{\partial Y_i}/\partial y)_w$. At the same time, the component i is transported away from the interface by the normal current at the rate $(\rho V)_w Y_{F_w}$ in the gas, and $(\rho V)_w Y_{i-}$ in the vaporizing solid wall. The rate of production of the component i by the surface reaction is

$$J_{iw}=-\rho_w D(\partial Y_i/\partial y)_w+(\rho V)_w(Y_{F_w}-Y_{i-}) \tag{A8}$$

where J_{iw} is the rate of production of the ith specie due to surface reaction. Now Y_{i-} is zero when the particular ith specie is not included among the vaporized gas mixture, or equals unity when the vaporized gas is entirely composed of the ith specie. This means that if the condensed phase is composed of pure fuel, $Y_{i-}=1$, if $i=$ fuel, while all other $Y_-=0$.

Condition A8 does not completely specify the boundary condition for specie conservation because the blowing rate is unknown and must be expressed by auxiliary analysis. In order to express the blowing (mass) rate, $(\rho V)_w$, in terms of other physical parameters, it is usually assumed that one may incorporate a pyrolysis relation, $\dot{r}=\dot{r}(T_w)$. An example is a simple Arrhenius function,

$$\dot{r}=A\exp(-E_w/RT_w) \tag{A9}$$

where A is the pre-exponential factor and E_w is the activation energy. Equation (A9) is called the pyrolysis equation and is valid for most polymer fuels.

Now T_w is the unknown. Because of the coupling nature of conditions at the wall, and the fact that the process must be self-sustaining, the case of a constant wall temperature is unrealistic. Experimentally, it is known that the wall temperature is related to either the wall blowing rate by Eq. (A9) or the wall mass fraction. Another auxiliary condition is now required. This is the energy balance at the surface.

The interface conservation of energy necessary to calculate the net rate of convective heat transfer to the solid is[2]

$$\dot{q}_-\equiv\lambda_p\left(\frac{\partial T}{\partial y}\right)_-=\lambda\left(\frac{\partial T}{\partial y}\right)_w+\rho_w\sum_{i=1}^{N}D_i h_i\left(\frac{\partial Y_i}{\partial y}\right)_w-(\rho V)_w\sum_{i=1}^{N}[Y_{iw}h_{iw}-Y_{i-}h_{iw-}] \tag{A10}$$

where $\dot{q}_-$ is the heat conducted into the solid.

For steady heat conduction into the solid it is easy to show [see Waldman et al. (1969)] that in terms of temperature, the boundary condition is

$$\left(\lambda\frac{\partial T}{\partial y}\right)_w=(\rho V)_w[c_{p-}(T_w-T_p)+L+(c_{p-}-c_p)T_w] \tag{A11}$$

Equation (A11) shows the coupling between the momentum and energy boundary conditions at the surface. [With this equation, the parameter B is defined as shown in Eq. (8f).]

At the freestream, the boundary conditions on velocity, temperature and species are known. They may be written as $y\to\infty$

$$u=u_e \tag{A12a}$$

$$Y_i=Y_{\mathrm{Ox}_e}\ \text{(known)} \tag{A12b}$$

$$T=T_e\ \text{(known)} \tag{A12c}$$

Equations (A8–A12) now provide sufficient boundary conditions necessary for the solution of the conservation equations.

References

[1] Lees, L., "Convective Heat Transfer with Mass Addition and Chemical Reactions," *Combustion and Propulsion: Third AGARD Colloquium*, Pergamon Press, New York, 1958, pp. 451–497.

[2] Chung, P. M., "Chemically Reacting Non-Equilibrium Boundary Layers," *Advances in Heat Transfer*, Vol. 2, Academic Press, London, 1965, pp. 110–268.

[3] Dorrance, W. H., *Viscous Hypersonic Flow*, McGraw-Hill, New York, 1962.

[4] Green, L., Jr., "Introductory Considerations of Hybrid Rocket Combustion," *Heterogeneous Combustion Progress in Aeronautics and Astronautics*, Vol. 15, Academic Press, New York, 1964, pp. 451–484.

[5] Tsugé, S. and Fujiwara, Y., "Fine Structure of Hybrid Combustion," *Astronautica Acta*, Vol. 14, 1969, pp. 327–335.

[6] Williams, F. A., *Combustion Theory*, Addison-Wesley, Reading, Pa., 1965.

[7] Liu, T. M. and Libby, P. A., "Boundary Layer at Stagnation Point with Hydrogen Injection," *Combustion and Science Technology*, Vol. 2, 1970, p. 131.

[8] Waldman, C. H., Cheng, S. I., Sirignano, W. A., and Summerfield, M., "Theoretical Studies of Diffusion Flame Structure," AFOSR Scientific Report 69-0350 TR, and AMS Report 860, 1969, Princeton Univ., Princeton, N.J.

[9] Chung, P. M., "Heat Transfer in Chemically Reacting Gases," *Advanced Heat Transfer*, edited by B. T. Chao, University of Illinois Press, Urbana, Ill., 1969, pp. 319–338.

[10] Penner, S. S. and Libby, P. A., "Convective Laminar Heat Transfer with Combustion for a Lewis Number of Unity," *Astronautica Acta*, Vol. 13, 1967, pp. 75–91.

[11] Kerzner, H., "Chemically Reacting Boundary Layer over a Vaporizing Surface," Ph.D. thesis, 1972, Univ. of Illinois, Urbana-Champaign, Ill.

[12] Libby, P. A. and Pierucci, M., "Laminar Boundary Layer with Hydrogen Injection Including Multicomponent Diffusion," *AIAA Journal*, Vol. 2, No. 12, Dec. 1964, pp. 2118–2126.

[13] Emmons, H. W., "Film Combustion of Liquid Fuels," *Zeitschrift für Agnewandte Mathematik und Mechanik*, Band 36, Heft 1/2, 1956, pp. 60–70.

[14] Chen, T. N. and Toong, T. Y., "Laminar Boundary Layer Wedge Flows with Evaporation and Combustion," *Heterogeneous Combustion Progress in Astronautics and Aeronautics*, Vol. 15, Academic Press, New York, 1964, pp. 643–664.

[15] Smoot, L. D. and Price, C. F., "Regression Rate of Mechanisms of Nonmetalized Hybrid Fuel Systems," *AIAA Journal*, Vol. 3, No. 8, Aug. 1965, pp. 1408–1413.

[16] Smoot, L. D. and Price, C. F., "Pressure Dependence of Hybrid Fuel Regression Rates," *AIAA Journal*, Vol. 5, No. 1, Jan. 1967, pp. 102–106.

[17] Kosdon, F. J. and Williams, F. A., "Pressure Dependence of Nonmetalized Hybrid Fuel Regression Rates," *AIAA Journal*, Vol. 5, No. 4, April 1967, pp. 774–778.

[18] Kumar, R. N. and Stickler, D. B., "Polymer-Degradation Theory for Pressure-Sensitive Hybrid Combustion," *Thirteenth Symposium on Combustion*, The Combustion Inst., Pittsburgh, Pa., 1970, pp. 1059–1072.

DECEMBER 1973 AIAA JOURNAL VOL. 11, NO. 12

Influence of Gradient of Velocity upon the Resonant Radiative Transfer in Plasma Flows

P. VALENTIN,* M. PINEGRE,† M. TERRIER‡
Commissariat à l'Energie Atomique, Sevran, France

The aim of this work is to estimate the influence of a velocity gradient upon the resonant radiative transfer and to propose an approximate analytical solution of the transfer equation. The radiative population rate of the resonant states is shown to be notably influenced by a velocity gradient of the same order as that found in a boundary layer along a wall in a supersonic flow. Thus this rate appears to be from one to three orders of magnitude smaller than in the case of zero gradient.

Nomenclature

A_{rf}	= Einstein coefficient for spontaneous emission of the resonance lines
B	= population rate due to the photons which are emitted in the freestream plasma
B_{fr}	= Einstein coefficient for absorption
C	= velocity of light
I_ν	= specific intensity of the radiation at ν
k_ν	= spectral absorption coefficient per unit length at ν
L	= boundary-layer thickness
l	= distance normal to the freestream boundary
l^*	= dimensionless length (Sec. V)
L'	= thickness of the plasma
$l' = L' - L$	= thickness of the homogeneous plasma
N	= density number
S	= line strength
U	= velocity in the streamwise direction
u', v', w'	= coordinate system (Fig. 4)
Z	= distance normal to the wall
α	= $(1/\delta\nu_D)^2$
β	= expression defined in Eq. (10)
β_0	= value of β for zero gradient
β'	= expression defined in Eq. (42)
γ	= $\lvert(1/C)\,\partial U/\partial Z\rvert$
Δ	= population rate due to the photons which are emitted in the nonhomogeneous plasma
$\delta\nu_D$	= (half) half-width doppler
θ, ϕ	= angular coordinate system (Figs. 2 and 4)
ν	= radiation frequency
ξ, η, ζ	= coordinate system (Fig. 2)
τ	= lifetime = $1/A_{rf}$
χ	= dimensionless frequency

Subscripts

e	= freestream value
f	= ground state
m	= metastable state of A_1
r	= resonant states

Received December 20, 1972; revision received July 9, 1973.
Index categories: Radiatively Coupled Flows and Heat Transfer; Atomic, Molecular, and Plasma Properties; Radiation and Radiative Heat Transfer.

* Professeur à l'Université de Rouen.
† Maître-Assistant à l'Université de Rouen, détaché au C.E.A.
‡ Assistant à l'Université de Rouen.

I. Introduction

IN many studies on plasma-jets, electron-ion recombination rate coefficients of homogeneous decaying plasmas are often used in the species (electrons and ions) conservation equations.